

## Modern microcenter heat explosion model

A V Kalenskii<sup>1,2</sup>, V G Kriger<sup>1,\*</sup>, I Yu Zykov<sup>1</sup> and M V Anan'eva<sup>1</sup>

<sup>1</sup>Solid state department, Kemerovo State University, Kemerovo 650043, Krasnaya 6, Russia

E-mail: kriger@kemsu.ru

**Abstract.** Modernization and investigation of the microcenter heat explosion model of the energetic materials initiated by the pulse radiation was made in this paper. Absorptivity of aluminium nanoparticles in PETN-matrix was calculated and was taken into account. Dependences of the absorptivity on the particles' sizes and wave length of irradiation was also taken into account. It was shown that the particle's radius, which corresponds to the absorption maximum, and the peak value both depend on the irradiation wave length. For the first harmonic of the ND:YAG laser the absorption maximum corresponds to the nanoparticle's radius 100 nm, for the second harmonic to the radius it is 44 nm. The peak value increases from 0.2942 to 0.7064. Dependences of the critical initiation energy densities on the metal inclusions' radii were calculated for the energetic materials. It was concluded that the RDX – aluminium composite is the perspective material to use in optic detonator especially for the second harmonic of the ND:YAG laser.

### 1. Introduction

The microcenter model of the energetic materials explosion initiation is based on the assumption that in the sample's volume there are inclusions with the radii about 100 nm effectively absorbing laser irradiation. It is supposed that the main result of absorption is the inclusions heating which cause the growth of the temperature of its neighborhood. The temperature growth leads to a reaction zone formation. The cross section of the light absorption by the inclusion is thought to be equal its geometrical cross-section [1]. It means that the absorptivity  $Q_{\text{abs}}=1$ . First the model was proposed to explain the regularities of the azide heavy metals explosive decomposition process [2-3]. At the same time in works [4-6] was proposed mechanism of the branched chain reaction, which allowed to describe quantitatively the regularities of the silver azide explosive decomposition initiated by the action of the laser pulse [6-8].

In works [9-10] it was shown that the additions of aluminium nanoparticles allow to decrease the critical initiation energy density of PETN in two orders of magnitude. Due to this fact it was proved the role of the small inclusions absorbing the irradiation in the samples of the secondary explosive materials. It was shown the possibility of use of the secondary explosive materials, containing nanosized additives, as a percussion cap for the optical initiation systems. To find the material and the sizes of the additives giving the minimal critical initiation energies, it is necessary to simulate the initiation process according the materials properties, which were supposed previously negligible. The aim of this work is to work out and investigate the modern variation of the microcenter heat explosion model taking into account the absorptivities of the metal nanoparticles.



## 2. Microcenter model in case of pulse laser initiation

In case of pressed pellet of PETN, containing nanosized aluminium particles, the light got into the sample undergoes multiple reflections at the grain boundaries. As the reflections have the chaotic character the illumination are averaged over all the directions, this allows to use (as it was done in works [1, 11]) spherical symmetry and suppose the inclusion is also a sphere. The main processes taking into account in the presented model is the heating of nanoparticle by the irradiation, heat removing into the energetic material, and chemical heat-generating reaction of the explosive's decomposition. The processes are described by the equations set:

$$\begin{aligned}\frac{\partial T}{\partial t} &= \alpha \cdot \left( \frac{\partial^2 T}{\partial x^2} + \frac{2}{x} \cdot \frac{\partial T}{\partial x} \right) + k_0 \frac{nQ}{c} \cdot \exp\left(-\frac{E}{k_B T}\right), x > R \\ \frac{\partial n}{\partial t} &= -k_0 n \cdot \exp\left(-\frac{E}{k_B T}\right), x > R \\ \frac{\partial T}{\partial t} &= \alpha_M \cdot \left( \frac{\partial^2 T}{\partial x^2} + \frac{2}{x} \cdot \frac{\partial T}{\partial x} \right), x < R \\ \frac{\partial n}{\partial t} &= 0, n = 0, x < R\end{aligned}\quad (1)$$

the boundary condition is  $x = R$ :

$$J - c_M \alpha_M \cdot \frac{\partial T}{\partial x} \Big|_{x \rightarrow R-0} + c \alpha \cdot \frac{\partial T}{\partial x} \Big|_{x \rightarrow R+0} = 0 \quad (2)$$

where  $T$  is temperature,  $E$  – decomposition activation energy,  $k_0$  - preexponential factor,  $Q$  – thermal effect of the reaction,  $\alpha$  and  $\alpha_M$  are the coefficients of thermal conductivity of the matrix and inclusion materials,  $R$  in the inclusion radius,  $c$  и  $c_M$  is the volumetric heat capacity of the matrix and inclusion material,  $n$  is the share of undecomposed explosive, and  $J(t)$  is the absorbed density of the laser pulse radiation power. For the simulation the following parameters were used:  $c = 2.22 \text{ J}/(\text{cm}^3\text{K})$ ,  $c_M = 2.7 \text{ J}/(\text{cm}^3 \cdot \text{K})$ ,  $E = 165 \text{ kJ}/(\text{mol} \cdot \text{K})$ ,  $k_0 = 1.2 \cdot 10^{16} \text{ s}^{-1}$ ,  $\alpha = 1.1 \cdot 10^{-3} \text{ cm}^2\text{s}^{-1}$ ,  $\alpha_M = 0.97 \text{ cm}^2\text{s}^{-1}$ ,  $Q = 9.64 \text{ kJ}/\text{cm}^3$  [11]. The dependence of the laser pulse radiation power on time is close to the normal distribution function [12]. Taking as a reference time position of maximum intensity of the pulse, we obtain for value  $J(t)$  the expression [13]:

$$J(t) = \sqrt{\pi} \cdot Q_{abs} R^2 k_i H_0 \cdot \exp\left(-k_i^2 t^2\right) \quad (3)$$

where  $k_i = 8.325 \cdot 10^7 \text{ s}^{-1}$  is the parameter determining the pulse duration,  $H_0$  is the averaged density of energy during a single pulse;  $Q_{abs}$  is the absorption efficiency equal to the ratio of intensities of radiation absorbed and incident on the inclusion, meanwhile its value depends both on the inclusion radius and radiation wavelength. Multipliers of Eq. (3) normalize the integral of  $J(t)$  over time by  $H_0$ . Numerical solution of model (1)–(3) was made using variable-pitch grid. A step in the neighborhood of the inclusions with the radii  $R \geq 30 \text{ nm}$  was no more than  $1/20$  of the thickness of the inert substance heated during the pulse ( $\sqrt{2\alpha/k_i}$ ), then the cell size increased exponentially, so that the total thickness of the surrounding material was no less than  $8R$ . For the pulse duration used in the simulation, the heating length was equal to  $\approx 50 \text{ nm}$  and the size of cells near the inclusion was about  $2.5 \text{ nm}$ . Step of grid inside the inclusion exceeded the step outside in  $\sqrt{\alpha_M/\alpha}$  times. The cell on the bound inclusion-matrix contained both the matrix material and the inclusion material with the

thickness equal to the half step of the grid. For the mentioned characteristics the size of the cell inside the inclusion was about 10nm that is near to the thickness of the light absorption layer. This layer does not exceed 10 nm for the majority of metals. For the inclusions with the radii  $20 \geq R > 10$  nm one cell was used inside the inclusion and next there was a cell containing the boundary inclusion-matrix. For the inclusions with the radii  $R \leq 10$  nm there was one cell included all the inclusion material, boundary inclusion-matrix and the matrix material. This method allows to make a reasonable consideration of light absorption by means of boundary condition (2) [14].

The ordinary differential equation set got after the dividing of the space into cells was solved by the Runge — Kutta method of 1–5 orders with a variable time step. A relative error at an integration step does not exceed  $10^{-9}$ , whereas the integral relative error estimated by the precision of performance of the law of conservation of energy did not exceed  $2.5 \cdot 10^{-5}$ .

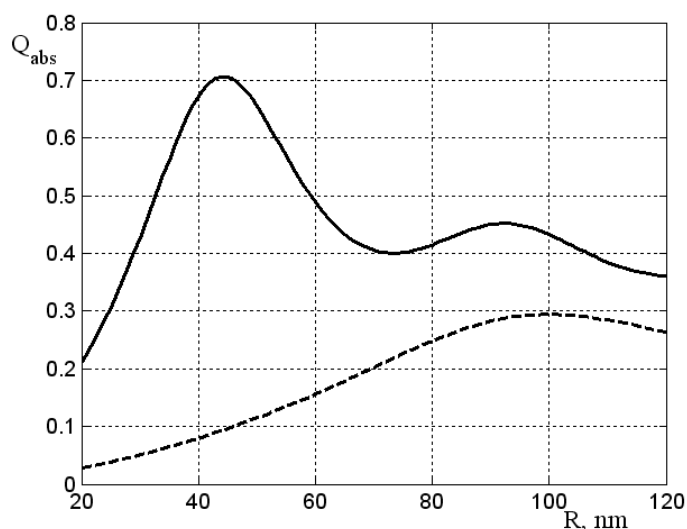


**Figure 1.** Calculated dependences of the absorptivities ( $Q_{abs}$ ) on the aluminium nanoparticles' radii for the first (1064 nm) and the second (532 nm) harmonics of the of the ND:YAG laser.

### 3. Influence of the metal nanoparticles' absorptivity on the critical parameters of initiation

Theories of absorption and scattering of the electromagnetic radiation by the small particles are known for enough long time. In case of the spherical particle the Mie's theory was proposed. The method of calculation was described in work [15-16]. Figure 1 shows the calculated dependences of the absorptivities ( $Q_{abs}$ ) on the aluminium nanoparticles' radii in the PETN-matrix for the first (1064 nm) and the second (532 nm) harmonics of the of the ND:YAG laser. The refractive index of aluminium at the wavelengths of 1064 nm and 532 nm was  $m_i=0.978 - 8.030i$  and  $0.5559 - 4.8553i$ , respectively [17]. The curves have maximums, whose positions are determined mainly by the radiation wavelength. In the area of the radii smaller than the radius of the maximum the curve falls to zero. In the area of the radii greater than the radius of the maximum the arrival at the oscillation plateau occurs.

The influence of the wavelength within the Mie theory is due to the fact that the arguments of the special functions for which expansion is carried out depend on the wavelength and the complex refractive index. If the refractive index  $m_i$  does not depend on the wavelength, the dependences  $Q_{abs}(R/\lambda)$  would coincide. The real and imaginary parts of  $m_i$  can change by several times if the wavelength varies, which complicates the calculations. In the case of aluminium, in the transition from the first to the second harmonic of the ND:YAG laser, the real part of the refractive index decreases by 1.76 times and the imaginary part decreases by 1.65 times [17]. Because of both factors, the absorption

efficiency maximum is shifted toward the small diameters of the inclusions (see Figure. 1). For the first harmonic the maximum is observed when inclusion's radius is 100 nm, for the second harmonic when the inclusion's radius is 44 nm. Furthermore, the maximum amplitude increases from 0.2942 at a wavelength of 1064 nm up to 0.7064 at a wavelength of 532 nm.

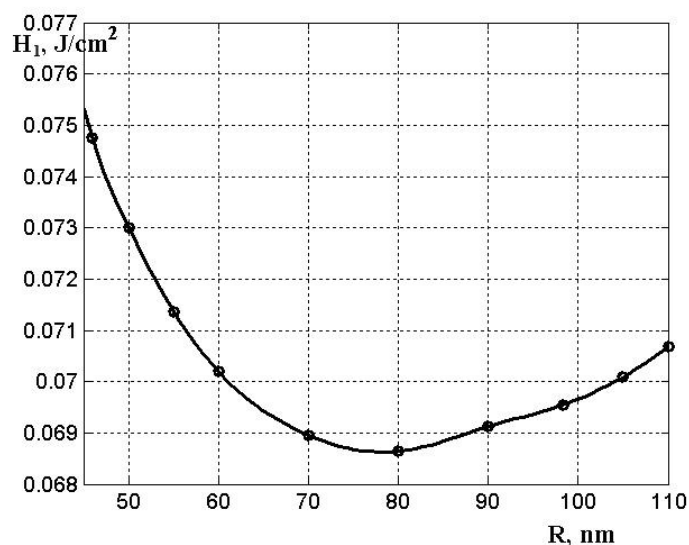


**Figure 2.** Calculated dependence of the critical initiation energy density on the radius of aluminum inclusions in the PETN matrix without taking into account the absorption particularities.

Figure 2 shows the calculated dependence of the critical initiation energy density on the aluminium nanoparticle's radius in PETN without taking into account the absorption particularities ( $Q_{\text{abs}} = 1$ ). The value of the critical initiation energy density does not depend on the wavelength in the area of the impurity absorption of the matrix, this statement includes the values of the first and the second harmonic of the ND:YAG laser. The curve's minimum is located in the radii range 70-80 nm. The minimum appears due to the heating particularities of the spherical nanoparticle. The maximum temperature change  $\delta T$  of the inclusion with the radius  $R$  during the heating by the laser pulse with the energy density  $H$  might be calculated using the equation

$$\delta T = \frac{HR/4c}{Rh + h^2 + R^2/K^2} \quad (4)$$

where  $K = \sqrt{3c/c_M}$  – dimensionless coefficient, which considers the ratio of the coefficients of thermal conductivity of the matrix and inclusion,  $h = \sqrt{\alpha t_i}$  – thickness of the heated layer during the time of the pulse duration  $t_i$ . The radius of the most heated inclusion is equal to  $Kh$ , this value depends on the pulse duration. It turns out that the dependence of the maximum temperature of the heating on the inclusion radius in the inert matrix has the maximum, those position approximately corresponds to the minimum on the dependence of the critical initiation energy.

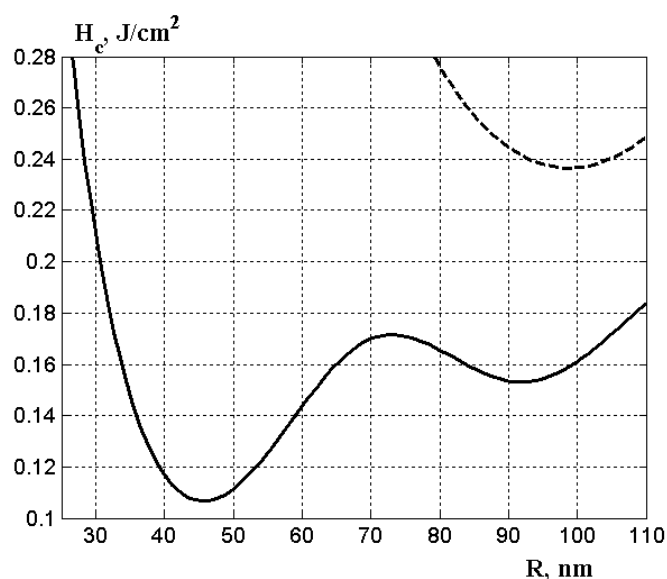


**Figure 3.** Dependence of the critical initiation energy density on the radius of the aluminium inclusions in the PETN matrix, calculated for the radiation wavelengths 532 nm (solid line) and 1064 nm (dashed line).

Critical energy density of the irradiation, which is expected to be found in an experimental research, is equal to the composition of the values presented on the pictures 1 and 2:  $H_c(R) = H_1(R) / Q_{abs}(R, \lambda)$ . Curve  $H_c(R)$  for aluminium nanoparticles in PETN for the wavelengths 1064 and 532 nm presented on figure 3. Consideration of the absorptivity dependence on the wavelength leads to three main consequences. First of all, according to the experimental data [11] there is a spectral dependence of the critical energy density on the wavelength of the initiating pulse. Then, the minimum depth on the curve, describing the dependence of the critical energy density on the inclusion's radius, changes. The minimal energy density increases from 68.7 mJ/cm<sup>2</sup> (if the absorptivity is not taken into account) to 236.6 mJ/cm<sup>2</sup> ( $\lambda=1064$  nm) and 106.6 mJ/cm<sup>2</sup> ( $\lambda=532$  nm). This is due to the fact that the aluminium absorptivities are smaller than 1 for all particles' sizes and all researched (significant) wavelengths (figure. 1). And the last, the minimum's position changes from 79 nm (for  $Q_{abs} = 1$ ) to 99 nm and 45 for the first and second harmonic of the ND:YAG laser correspondingly (figure. 3). So the minimum position is determined mainly by the optimal absorption conditions. Thus, the model predicts decrease of the critical energy density in case the initiating wavelength decreases.

The minimal critical energy densities calculated for the first and the second harmonic of the ND:YAG laser differ in 2.2 times, this result is in good agreement with the experiment (for the first harmonic – 1.15 J/cm<sup>2</sup>, for the second harmonic – 0.7 J/cm<sup>2</sup>) where they differ in 1.65 times.

This calculations allows to conclude that the RDX – aluminium composite is the perspective material to use in optic detonator especially for the second harmonic of the ND:YAG laser. This work was supported by Ministry of Education and Science of the Russian Federation (governmental project No. 2014/64).

## References

- [1] Burkina R S, Morozova E Yu and Tsipilev V P 2011 Initiation of a reactive material by a radiation beam absorbed by optical heterogeneities of the material *Combust., Expl., Shock Waves* **47(5)** 581–90
- [2] Kriger V G and Kalenskii A V 1995 Initiation of heavy metal azides by pulse radiation *Chem. Phys. Rep.* **14(4)** 556–64
- [3] Kriger V G and Kalenskii A V 1996 The effect of crystal size on initiation of decomposition of heavy metal azides by pulse radiation, *Chem. Phys. Rep.* **15 (3)** 351–58
- [4] Kriger V G, Kalensky A V and Zvekov A A 2012 Relaxation of electronically excited products of solid-state reactions in the crystal lattice, *Russ. J. Phys. Chem. B* **48 (1)** 15–18
- [5] Kalenskii A V, Bulusheva L G, Kriger V G and Mazalov L N 2000 Quantum chemical cluster modeling of boundary conditions for metal azides, *J. struct. Chem.* **41 (3)** 495–98
- [6] Kalenskii A V, Anan'eva M V, Kriger V G and Zvekov A A 2014 Rate constant of capture of electron charge carriers on a screened repulsive center, *Russ. J. Phys. Chem. B* **8 (2)** 131–35
- [7] Kriger V G, Kalenskii A V, Zvekov A A, Borovikova A P and Grishaeva E A 2012 Determining the width of the reaction wave front in the explosive decomposition of silver azide *Combust., Expl., Shock Waves* **48 (4)** 488–95
- [8] Kriger V G, Kalenskii A V, Zvekov A A and Tsipilev V P 2009 Explosive decomposition of silver azide single crystals for various diameters of the irradiated area. *Combust., Expl., Shock Waves* **45 (6)** 729–31
- [9] Aduiev B P, Belokurov G M, Nurmukhametov D R and Nelyubina N V 2012 Photosensitive material based on PETN mixtures with aluminum nanoparticles *Combust., Expl., Shock Waves* **48 (3)** 361–66
- [10] Aduiev B P, Nurmukhametov D R, Tsipilev V P and Furega R I 2013 Effect of ultrafine Al-C particle additives on the PETN sensitivity to radiation exposure *Combust., Expl., Shock Waves* **49 (2)** 215–18
- [11] Aduiev B P, Nurmukhametov D R, Furega R I, Zvekov A A and Kalenskii A V 2013 Explosive decomposition of PETN with nanoaluminum additives under the Influence of pulsed laser radiation at different wavelengths *Russ. J. Phys. Chem. B* **7(4)** 453 – 56
- [12] Kriger V G, Kalenskii A V, Zvekov A A 2010 Determining the onset of mechanical failure of silver azide crystals initiated by a laser pulse *Combust., Expl., Shock Waves* **46 (1)** 60–63
- [13] Kriger V G, Kalenskii A V, Zvekov A A, Anan'eva M V and Borovikova A P 2009 A Diffusion model of chain-branching reaction of the explosive decomposition of heavy metal azides *Russ. J. Phys. Chem. B* **3 (4)** 636–40
- [14] Kriger V G, Kalenskii A V, Zvekov A A, Zykov I Yu and Nikitin A P 2013 Heat-transfer processes upon laser heating of inert-matrix-hosted inclusions *Thermophysics and Aeromechanics* **20 (3)** 367–74
- [15] Kriger V G, Kalenskii A V, Zvekov A A, Zykov I Yu and Aduiev B P 2012 Effect of Laser Absorption efficiency on the heating temperature of inclusions in transparent media *Combust., Shock Waves* **48 (6)** 705 – 8
- [16] Kalenskii A V, Zvekov A A, Anan'eva M V, Zykov I Yu, Kriger V G and Aduiev B P 2014 Laser wavelength influence on the critical density of initiation energy of energetic materials *Fizika Goreniya i Vzryva* **50 (3)** 98–104
- [17] Zolotarev V M, Morozov V N and Smirnova E V 1984 *Optical Constants of Natural and Technical Media* (Leningrad.: Khimiya) p. 216